International Journal of Automation and Computing 17(4), August 2020, 599-609
DOI: 10.1007/s11633-017-1064-0

Optimal Design of Fuzzy-AGC Based on PSO & RCGA to Improve Dynamic Stability of Interconnected Multi-area Power Systems

Ali Darvish Falehi

Department of Electrical Engineering, Shahid Beheshti University, Tehran 1983963113, Iran

Abstract: Quickly getting back the synchronism of a disturbed interconnected multi-area power system due to variations in loading condition is recognized as prominent issue related to automatic generation control (AGC). In this regard, AGC system based on fuzzy logic, i.e., so-called FLAGC can introduce an effectual performance to suppress the dynamic oscillations of tie-line power exchanges and frequency in multi-area interconnected power system. Apart from that, simultaneous coordination scheme based on particle swarm optimization (PSO) along with real coded genetic algorithm (RCGA) is suggested to coordinate FLAGCs of the all areas. To clarify the high efficiency of aforementioned strategy, two different interconnected multi-area power systems, i.e., three-area hydro-thermal power system and five-area thermal power system have been taken into account for relevant studies. The potency of this strategy has been thoroughly dealt with by considering the step load perturbation (SLP) in both the under study power systems. To sum up, the simulation results have plainly revealed dynamic performance of FLAGC as compared with conventional AGC (CAGC) in each power system in order to damp out the power system oscillations.

Keywords: Power system dynamic stability, fuzzy logic automatic generation control (FLAGC), particle swarm optimization (PSO), real coded genetic algorithm (RCGA), simultaneous coordination scheme.

1 Introduction

In past decades, the diurnally sustaining growths of electrical power systems in categorize and plexus as well as expansion of the interconnected system were turned to prominent issues related to the electric quality and dynamic stability[1−4]. The power systems dynamic behavior can be extremely affected by any operating condition change and also perturbation occurrence that may lead to heightening the amplitude of oscillations and consequently loss of synchronism[5]. Toward this subject, unraveling this issue is functional responsibility of automatic generation control (AGC). This momentousness is due to its factual and secure operation in interconnected power systems to abate the system frequency and tie-line power exchange deviations during the load perturbations occurrence[6]. In other words, AGC system pursues three prominent targets in the multi-machine systems:

1) The steady state errors of frequency must be annihilated. 2) The tracking process must be appropriately done without increase of oscillations during the load disturbances. 3) The oscillations of the tie-line power along with frequency deviations must be kept down.

In last years, AGC has been one of the emphasized subjects related to the interconnected power systems that many different approaches and apparatuses have been offered for controlling this systems[7−9]. As might be expected, different disturbances occurrence in power system irrefutably has particular responses, but then, an effectual controller and application strategy against the different operating conditions are unavoidable.

Fuzzy controllers have been successfully implemented in many different nonlinear systems whose actions are extremely intricate to be modeled[10−12]. Power system is one of the nonlinear systems, thus engagement of the fuzzy logic controller (FLC) could be a good solution. This is because the application of FLC has been suggested in designing of fuzzy logic automatic generation control (FLAGC).

The most prominent held forth controllers have been constructed by using of FLC. Mamdani approach, one of the important fuzzy solution approaches, is practically and widely used. To optimally tune the FLAGCs′ parameters, it is imperative that an effective optimization technique to be utilized for the problem. Several conventional methods have been employed to tune the controllers′ parameters. The majority of them are based on the pole placement strategy[13, 14], eigenvalues[15, 16], residue compensation[17], as well as the current control strategy. It must be note that, such tactics are very time consuming, i.e., they are repetitive and need onerous computational burden with sluggish convergence. Meanwhile, the process is sensitive that may be trapped in local minima and also an optimal result can not be obtained[18]. The progressive approaches

Research Article
Manuscript received May 9, 2016; accepted August 8, 2016; published online April 19, 2017
Recommended by Associate Editor Giuliano Premier

provide an appropriate bed to search for the optimum solutions via some sort of directed random search operation[19]. Seeking a good solution without foregoing problem perception is suitable trait of the evolutionary approaches.

More recently, miscellaneous stochastic optimization approaches including: simulated annealing (SA), genetic algorithm (GA), differential evolution (DE), particle swarm optimization (PSO) and the same have been utilized by academic researchers to unravel the different optimization problems of electrical engineering. Whereas, PSO and real coded genetic algorithm (RCGA) techniques can produce excellent solution within short computation time and stable convergence characteristic[20, 21]. In fact, PSO is a stochastic global optimization strategy on the basis of swarm features namely fish and bird schooling in nature[22]. Also, GA is another kind of stochastic techniques which operates in accordance with natural selection mechanism and fittest survival in biological systems[21].

Due to high proficiency of PSO and RCGA techniques in unraveling the nonlinear and high-dimensional objectives, both of them have been employed to solve the problem of optimization. In this paper, FLAGC alongside of an effectual approach based on PSO and RCGA techniques have been taken into account so that the oscillation of the system frequency as well as the tie-line power exchange deviations in both studied power systems are alleviated. The step load perturbation (SLP) is considered in both the studied power systems to verify the efficiency and robustness of simultaneous coordination scheme.

To sum up, the obtained results of the simulations have clearly corroborated the robustness of aforesaid scheme alongside of FLAGCs′ dynamical performance as compared to conventional AGC (CAGCs) in each power system aimed at damping the power system oscillations.

2 Mamdani fuzzy logic applied to AGC

2.1 Fuzzy logic guideline

The principal part of the FLC is regulation of linguistic control rules related to two intentions of fuzzy implication and the structural rule of inference. The FLC performs converting the linguistic control system in accordance with a drastic arithmetical technique into an automatic control system. Two common variables that are chosen as inputs of fuzzy controller are error and error deviation. Here, area control error (ACE) and ACE derivative are fuzzy inputs.

2.2 Fuzzy controller structure definition

For this study, triangle type membership function which is shown in Figs. 1 and 2 is used to convert the inputs and output variable into linguistic control variables. The fuzzy quantities, such as negative big (NB), negative small (NS), zero (ZE), positive small (PS), positive big (PB), zero (ZZ), zero negative (ZN), zero positive (ZP), negative intermediate (NI), positive intermediate (PI), medium negative (MN), medium positive (MP), great negative (GN) and great positive (GP) are with related to membership functions. In this paper, the fuzzy control rules of state evaluation are applied which are similar to the institutional thinking of humans[12].

R^i: if C is A_{1i} and Δe is B_{1i}, then u is C_{1i}.

Here, e, Δe and u indicate the system variables error, error deviation and output, respectively. Also, A_{1i}, B_{1i} and C_{1i} are the linguistic values of the fuzzy variable to express the universe of discourse of the fuzzy set. For the inference mechanism, Mamdani′s sum-product technique has been applied. The fuzzy sets must be defuzzified to acquire the appropriate control output for the control system. Among the different defuzzification methods, centroid method is more common, which conforms to following equation[23].

$$\frac{\int u(x)x\mathrm{d}x}{\int u(x)\mathrm{d}x}. \tag{1}$$

The rule table accompanied by the littoral membership functions for the FLAGC structure is available in Table 1.

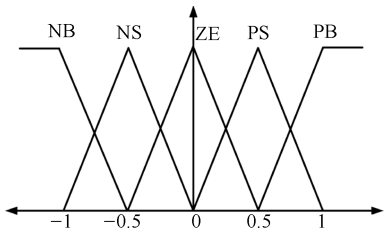

Fig. 1 Normalized membership function for ACE/Δ ACE

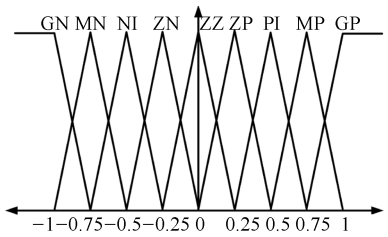

Fig. 2 Normalized membership functions of FLAGC output

Table 1 Lookup table of fuzzy rules

ΔACE/ACE	NB	NS	ZE	PS	PB
NB	GP	MP	PI	ZP	ZZ
NS	MP	PI	ZP	ZZ	ZN
ZE	PI	ZP	ZZ	ZN	NI
PS	ZP	ZZ	ZN	NI	MN
PB	ZZ	ZN	NI	MN	GN

2.3 Design of FLC for AGC controller

Currently, PI controller has been extensively engaged with industrial applications owing to its simple structure, low cost and easy design[9, 24−26]. In spite of these benefits, the proportional-integral (PI) type controller loses when the system is highly nonlinear and indistinct. Hence, retaining the benefits of PI controller and also injecting a fuzzy controller into it can be a good solution. This issue

causes FLAGC to be suggested which is shown in Fig. 3. In this structure, PI and proportional-derivative (PD) controllers are respectively used as output and input of fuzzy controller.

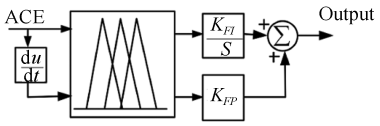

Fig. 3 Proposed PD-PI type fuzzy controller

3 Description of the implemented PSO and RCGA techniques

3.1 PSO technique

PSO, one of the exceptional optimization techniques, is developed by Kennedy et al.[27, 28]. This algorithm is drawn out in accordance with the behavior of organisms, such as fish schooling and bird flocking. Each particle casts around for the global minimum/maximum with traveling over the search space. By flying around the multi-dimensional search space, each particle adapts its position as situated with respect to its neighbors′ position[29]. PSO with high adaptability can properly control the balance between the global and local flexibility of the search space. In the current research, the concise process of this technique can be given as follows[30]:

1) Debut situation of gbest and pbest are not the same. Thus, using the several directions of *pbest* and *gbest*, all agents piecemeal will reach nearby the global optimum.

2) Adjustment of the agent position is perceived by the situation and velocity information. Even so, the approaches can be utilized to the distinct problem utilizing grids for XY position and its velocity.

3) Compatibility in searching procedure did not have any mismatching in searching procedures even if continuous and discrete variables are implemented with continuous axes and grids for XY situation and velocities.

4) The aforementioned declaration is based on application of only XY axis. This strategy can be easily utilized for n-dimensional problem. The amended situation and velocity of each particle can be computed via the current velocity and the distances from $pbest_{j,g}$ to $gbest_g$ as are available in following equation:

$$v_{j,g}^{(t+1)} = w \times v_{j,g}^{(t)} + c_1 + r_1 \times (pbest_{j,g} - x_{j,g}^{(t)}) + c_2 + r_2 \times (gbest_g - x_{j,g}^{(t)}) \quad (2)$$

$$x_{j,g}^{(t+1)} = x_{j,g}^{(t)} + v_{j,g}^{(t+1)} \quad (3)$$

$$v_g^{\min} \le v_{j,g}^{(t)} \le v_g^{\max} \quad (4)$$

where n is the particles number of swarm. m is the components number of the vectors v_j and x_j, t is the generation (iteration) number. $v_{j,g}^{(t)}$ is the g-th of the velocity component of particle j at generation t. c_1 and c_2 are positive factors, entitled cognitive $v_{j,g}^{(t)}$ and social criterions respectively. r_1 and r_2 are random numbers, uniformly scattered in (0, 1). $x_{j,g}^{(t)}$ is the g-th position component of particle j at iteration t. $pbest_j$ is the *pbest* of particle j. *gbest* is the *gbest* of the swarm. The inertia weight, w provides a balance between global and local explorations with less iterations on average to figure out an appropriate optimal solution. It can be presented as

$$w = w_{\max} - \frac{w_{\max} - w_{\min}}{iter_{\max}} \times iter \quad (5)$$

where $w_{\max}$ and $w_{\min}$ are the minimum and maximum weights, respectively. *iter* and $iter_{\max}$ are the present and maximum iteration numbers, respectively. The j-th particle of the swarm is stated by a d-dimensional vector $x_j = [x_{j,1}, x_{j,2}, \cdots, x_{j,d}]$ and its velocity rate is also stated by another d-dimensional vector $v_j = [v_{j,1}, v_{j,2}, \cdots, v_{j,d}]$. The best prior situation of the j-th particle is stated by $pbest_j = [pbest_{j,1}, pbest_{j,2}, pbest_{j,d}]$. The best particle′s index among all of the particles is also stated by the $gbest_g$. In PSO, any particle proceeds in the search space to try to find the best global minimum (or maximum). The updating procedure of velocity encompasses three parts; cognitive, momentum and social parts such that the proficiency of PSO depends upon the balance among these parts. The c_1 and c_2 have specified the relative pull of *pbest* and *gbest* and r_1 and r_2 assist in stochastically varying these pulls.

3.2 RCGA technique

The genetic algorithm (GA) is elicited from biological evolution introduced by Charles Darwin′s theory. The GA is operated based on natural selection, and also it had been subsequently developed by John Holland and his collaborators in the 1960s and 1970s. RCGA technique can be further explained as below[21]: Initialization: To initiate the RCGA optimization process, first population must be specified. The limitation of variables must be determined for optimization problem.

$$p = (p_{hi} - p_{lo})p_{norm} + p_{lo} \quad (6)$$

where P_{lo}, P_{ho} and P_{norm} are the fewest, topmost, and normalized amounts of the variables, respectively. Objective function: Every chromosome indicates a possible solution to optimize the fitness function. The fitness for every chromosome is dealt with by taking objective function. Eliminating the worst chromosomes, a new population will be created, that provided the most highly fit members are chosen to convey information to the next iteration.

$$chromosome = (variables) = [p_1, p_2, \cdots, p_{Nvar}] \quad (7)$$

$$cost = f(chromosome) = f(p_1, p_2, \cdots, p_{Nvar}). \quad (8)$$

Selection function: The selection function will determine which individuals can remain alive and convey genetic characteristic to the following generation. The selection function will also determine whose individuals are chosen for

crossing over. Genetic operator: Two fundamental factors are for GA process: crossover and mutation, which are engaged to generate new population to achieve the best solution. Crossover: Nucleus of genetic operation is crossover, which aids to acquire the new regions in the search space. In general, individuals′ pairs will be randomly taken from the population and each pair will be adjusted to allow them to be mated. Thus, where crossover occurs, is expressed as

$$\alpha = roundup(random \times Nvar). \tag{9}$$

Every pair of mates produces a child bearing some mix of two parents.

$$Parent_1 = [p_{m1}\ p_{m2}\ p_{m\alpha}\ p_{mNvar}] \tag{10}$$

$$Parent_1 = [p_{d1}\ p_{d2}\ p_{d\alpha}\ p_{dNvar}] \tag{11}$$

where m and d subscripts indicate the mom and the dad parents. The selected parents are thus merged to form the new variables that will emerge in the children:

$$PNew1 = p_{m\alpha} - \beta[p_{m\alpha} - p_{d\alpha}] \tag{12}$$

$$PNew2 = p_{d\alpha} + \beta[p_{m\alpha} - p_{d\alpha}] \tag{13}$$

where β is also a randomly chosen number between 0 and 1. The last step is to perfect the crossover with the rest of the chromosomes as before:

$$offspring_1 = [p_{m1}\ p_{m2}\ p_{New1}\ p_{mNvar}] \tag{14}$$

$$offspring_2 = [p_{d1}\ p_{d2}\ p_{New2}\ p_{dNvar}]. \tag{15}$$

Mutation: The principle of mutation factor is due to avoiding of missing the prominent information at a special situation in the decisions. With adding a normally distributed random number to the variable, uniform mutation will be obtained:

$$\acute{P}n = p_n + \sigma \times N_n(o, 1) \tag{16}$$

where σ = standard deviation of the normal distribution $N_n(0, 1)$ = standard normal distribution (mean=0 and variance = 1)

4 Presence of FLAGC in both interconnected power systems

4.1 Linearized model of three-area hydro-thermal system

The power system under study is constructed by three equal generating areas: two reheat thermal systems for Area 1 and Area 2, and also hydro system for Area 3. The linearized structure of hydro-thermal system presented in Fig. 4, has been simulated using Matlab/Simulink. Generation rate constraint (GRC) is chosen to be 3 percent per min for thermal areas, and also 270 percent per min for raising and 360 percent per min for the fewest generation of hydro area. A bias setting of B_i is chosen for both thermal and hydro areas. Meantime, the state-space equations of this system with FLAGC are presented as

$$\dot{x} = Ax + Bu + G \tag{17}$$

where G is a nonlinear term, and accordingly: the state variables and input for three-area interconnected power system including FLAGC are expressed as follows:

$$\begin{aligned} x^{\mathrm{T}} = [&\Delta f_1, \Delta P_{R1}, \Delta P_{G1}, \Delta P_{ref1}, \Delta x_1, \\ &\Delta f_2, \Delta P_{R2}, \Delta P_{G2}, \Delta P_{ref2}, \Delta x_2, \Delta f_3, \\ &\Delta P_{R3}, \Delta P_{G3}, \Delta P_{ref3}, \Delta x_3, \\ &\Delta P_{12}, \Delta P_{23}, \Delta P_{31}] \end{aligned} \tag{18}$$

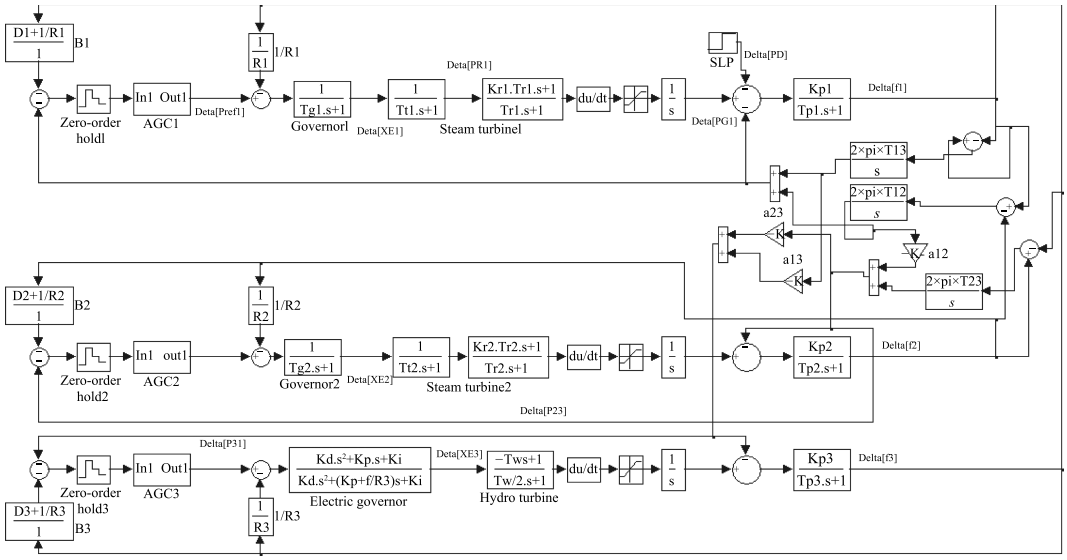

Fig. 4 Linearized model of three-area hydro-thermal power system

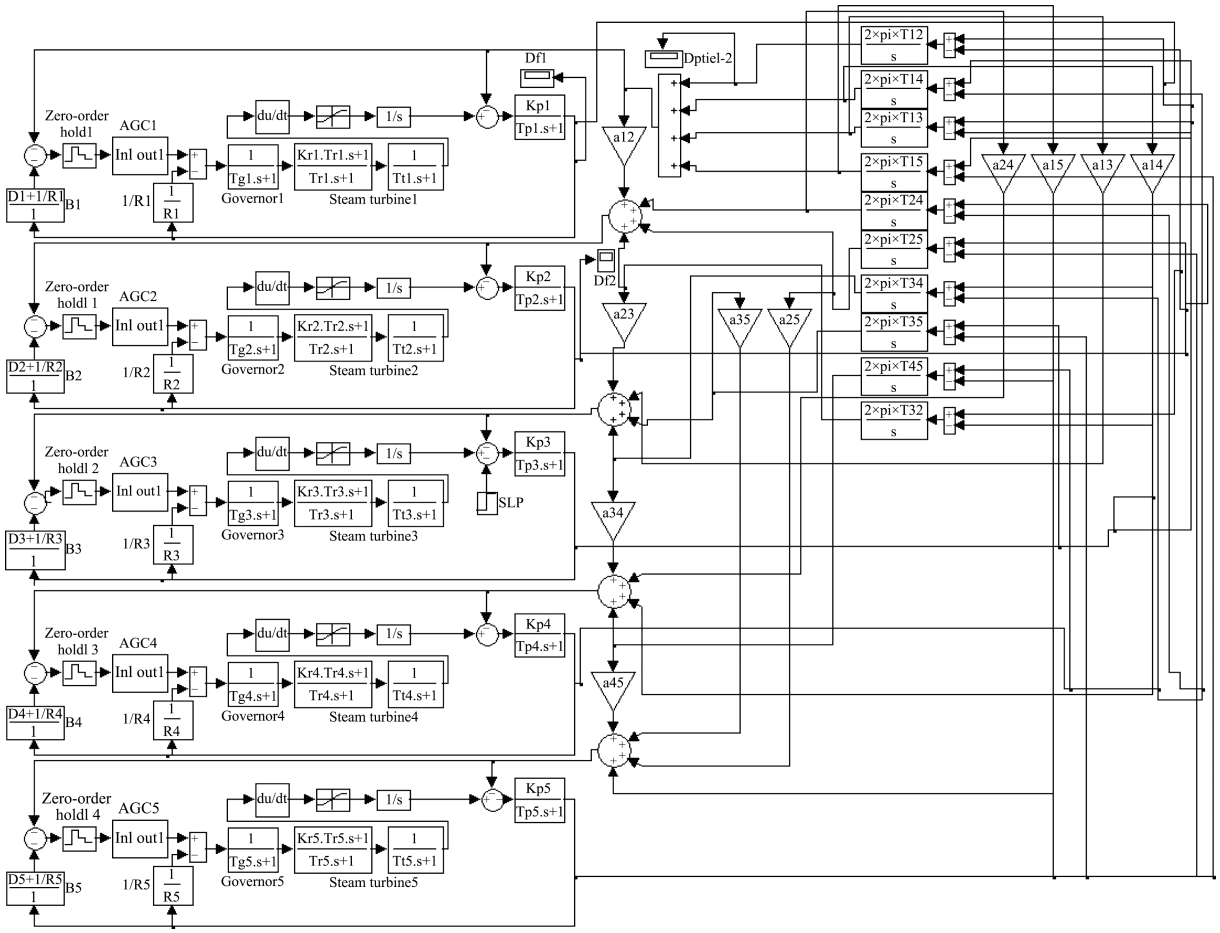

Fig. 5 Linearized model of five-area thermal power system

$$u^{\mathrm{T}} = [\Delta P_{D1}, \Delta P_{D2}, \Delta P_{D3}]. \tag{19}$$

For thermal areas: The frequency of each area of the power system can be represented by

$$\Delta f_{i(s)} = \frac{K_{pi}}{1 + sT_{pi}}[\Delta P_{Gi}(s) - \Delta P_{Di}(s) - \Delta P_i(s)]. \tag{20}$$

Accordingly, the fluctuations in turbine output power and mechanical power during steam reheat in each area have been respectively given in (21) and (22).

$$\Delta P_{Gi}(s) = \frac{1 + sK_{ri} \times T_{ri}}{T_{ri}} \Delta P_{Ri}(s) \tag{21}$$

$$\Delta P_{Ri}(s) = \frac{1}{1 + sT_{ti}} \Delta x_{Ei}(s). \tag{22}$$

Following that the output reference power of FLAGC in each area is drawn out as

$$\Delta P_{refi}(s) = -G_{FLAGC}[B_i(s)\Delta f_{i(s)} + \Delta P_i(s)]. \tag{23}$$

The governor valve position is afterward extracted by

$$\Delta x_{Ei(s)} = \frac{1}{1 + sT_{gi}}[\Delta P_{refi}(s) - R_i(s)^{-1}\Delta f_i(s)] \tag{24}$$

where i indicates thermal area number ($i = 1, 2$).

For hydro area: Similar to linearization of thermal areas, hydro area is linearized as

$$\Delta f_{3(s)} = \frac{K_{p3}}{1 + sT_{p3}}[\Delta P_{G3}(s) - \Delta P_{D3}(s) - \Delta P_3(s)] \tag{25}$$

$$\Delta x_{E3(s)} = \frac{K_d.s^2 + K_p.s + K_i}{K_d \times s^2 + (K_p + R_3^{-1}) \times s + K_i} [\Delta P_{ref3}(s) - R_3(s)^{-1}\Delta f_3(s)] \tag{26}$$

$$\Delta P_{G3}(s) = \frac{1 - sT_W}{1 + 0.5sT_W} \Delta P_{R3}(s) \tag{27}$$

$$\Delta P_{ref3}(s) = -G_{FLAGC}[B_3(s)\Delta f_{3(s)} + \Delta P_3(s)]. \tag{28}$$

Deviations of tie-line power can be expressed as

$$\Delta P_{12}(s) = \frac{2\pi T_{12}}{s}(\Delta f_1(s) - \Delta f_2(s)) \tag{29}$$

$$\Delta P_{23}(s) = \frac{2\pi T_{23}}{s}(\Delta f_2(s) - \Delta f_3(s)) \tag{30}$$

$$\Delta P_{31}(s) = \frac{2\pi T_{31}}{s}(\Delta f_3(s) - \Delta f_1(s)). \tag{31}$$

The final state variables related to each area of power system as well as the relevant state space equation can be

given as

$$\Delta P_1(s) = \Delta P_{12}(s) + \alpha_{31}\Delta P_{31}(s) \quad (32)$$

$$\Delta P_2(s) = \Delta P_{23}(s) + \alpha_{12}\Delta P_{12}(s) \quad (33)$$

$$\Delta P_3(s) = \Delta P_{31}(s) + \alpha_{23}\Delta P_{23}(s). \quad (34)$$

Other relevant parameters′ data are given in Appendix.

4.2 Linearized model of five area thermal power system

On the contrary, this system is carried out with consideration of five unequal generating areas[31]. The linearized structure of aforesaid system is presented in Fig. 5. The thermal systems are made up with single reheat turbine and GRC of percent per minute in each area. Other relevant parameters′ data are given in Appendix.

4.3 Configuration of conventional and proposed AGC

Annihilating of the area control error (ACE) of each interconnected system′s area is scheduled as the principal task of AGC system. That is to say, the system frequency and tie-line power exchange deviations are engaged as two key control variables, which deal with the AGC system. These variables are related with ACE by following equation[32, 33]:

$$ACE_i = \sum_j \Delta P_{tie-i,j} + B_i \Delta f_i \quad (35)$$

where B_i is frequency bias coefficient of ith area, Δf_i is frequency error of the i-th area, $\Delta P_{tie,i,j}$ is tie-line power deviation between the i-th area and the j-th area. The output of AGC controller in Laplace domain will be obtained by

$$G_{AGC,i}(s)ACE_i(s). \quad (36)$$

In this study, PI structure which is considered as conventional AGC. $G_{AGC}(s)$ for conventional and fuzzy controllers can be presented by the following equations:

$$G_{AGC,i}(s) = K_{CP,i} + s^{-1}K_{CI,i} \quad (37)$$

$$G_{FLAGC,i}(s) = K_{FP,i} + s^{-1}K_{FI,i}. \quad (38)$$

The parameters of conventional and fuzzy controllers which should be determined by PSO and RCGA techniques, include: K_{CP}, K_{CI}, K_{FP}, and K_{FI}. AGCs′ parameters in [34] are considered as non-coordinated parameters.

4.4 PSO technique

Simultaneous coordination of interconnected power systems′ AGCs: Many different approaches are introduced in relevant literatures such that the response performance of a control system, e.g., integral of time of absolute error (ITAE), integral of absolute of error (IAE), integral of squared error (ISE) and integral of time squared error (ITSE) can be appraised. For this simultaneous coordination scheme, F is suggested as total fitness function[35]:

$$\int_{t=0}^{sim} \left(\sum |\Delta f_i| + \sum |\Delta P_{tie-i,j}| \right) t \times \mathrm{d}t \quad (39)$$

$$F = \sum_{n=1}^{N_p} J_n \quad (40)$$

where t_{sim} indicates the simulation time range and N_p is the overall number of loading conditions. In this study, the PSO and RCGA techniques are applied to solve the optimization problem. The flowchart of the suggested optimization scheme is presented in Fig. 6. It is aimed to minimize "F". Therefore, the design problem is formulated as the following optimization problem:

$$\text{Min} \quad F. \quad (41)$$

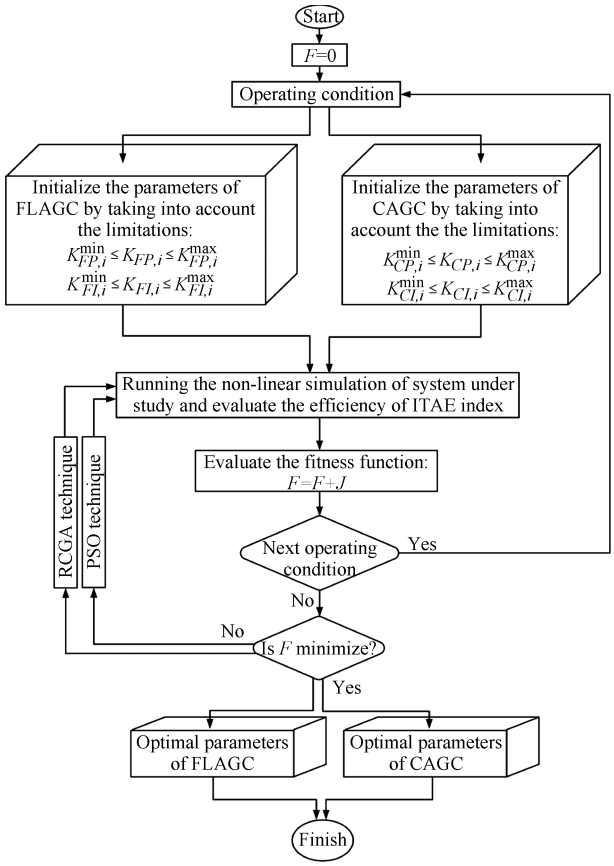

Fig. 6 Flowchart of the proposed optimization approach for both multi-area power systems

5 Simulation results

5.1 Three-area hydro-thermal power system

To inspect the effectiveness of simultaneous coordination scheme and also of FLAGC′s dynamic performance as compared with CAGC, it is considered that two SLP conditions happened in all areas of hydro-thermal power system. The simultaneous coordinated scheme for both the FLAGCs and

CAGCs is performed by evaluating the fitness function presented in (40). Optimal parameters of FLAGC and CAGC controllers are given in Tables 2 and 3. Also convergence of objective function values among PSO and RCGA is presented in Fig. 7. What is obvious from Fig. 8 is that all poles of this system with existence of FLAGCs have been situated at left complex semi-plane while some poles of this system with existence of CAGCs have been situated at right complex semi-plane. This reason has transparently revealed the high dynamic performance of FLAGC as compared with CAGC.

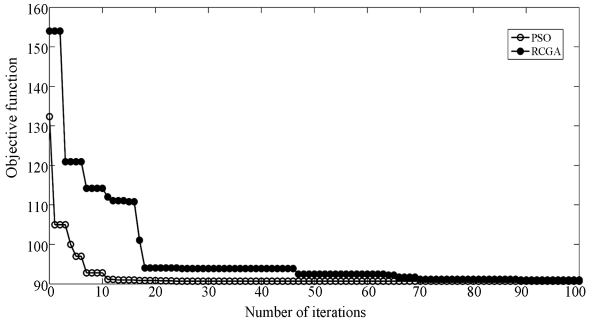

Fig. 7 Convergence of objective function values among PSO & RCGA

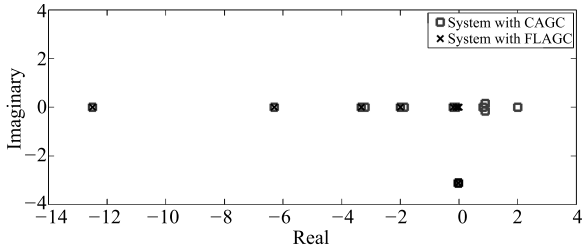

Fig. 8 System eigenvalues with presence of FLAGC and with CAGC

Table 2 Optimal parameters of hydro-thermal system′s FLAGCs

Area 1		Area 2		Area 3	
K_{FP1}	K_{FI1}	K_{FP2}	K_{FI2}	K_{FP3}	K_{FI3}
0.026 3	0.049 8	0.010 6	0.048 6	0.069 3	0.022 4

Table 3 Optimal parameters of hydro-thermal system′s CAGCs

Area 1		Area 2		Area 3	
K_{CP1}	K_{CI1}	K_{CP2}	K_{CI2}	K_{CP3}	K_{CI3}
0.290 3	0.150 9	0.909 5	0.500 6	0.058 7	0.091 8

Following results suggest the appropriate performance of FLAGC as compared with CAGC to augment the dynamic stability of hydro-thermal system.

Perturbation in Area 1.

The proposed coordination scheme is carried out under 3 percent SLP in Area 1 which is triggered at $t = 10$ s. As described above, PSO and RCGA techniques are applied to carry out the aforementioned proposed approach. The system response is shown in Fig. 9. Fig. 9 has transparently corroborated above mentioned citation.

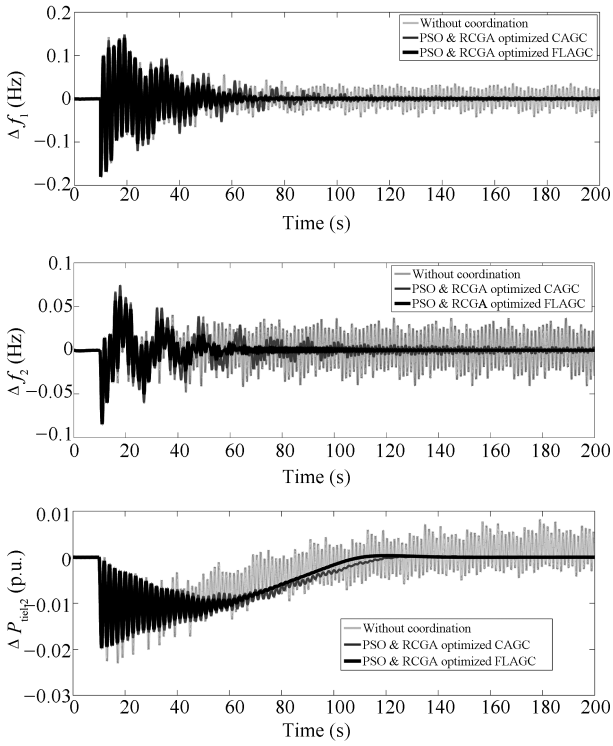

Fig. 9 Power system responses under 3 percent SLP in Area 1 at $t = 10$ s

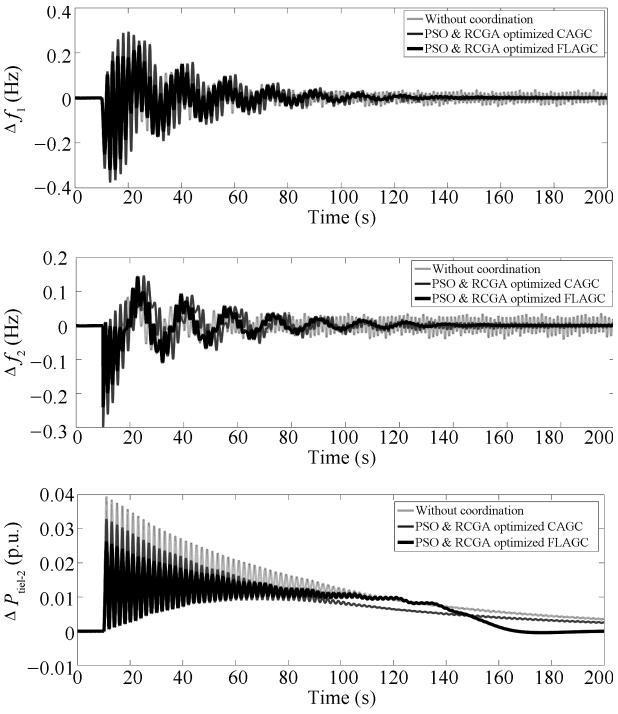

Fig. 10 Power system responses under 4 percent SLP in Area 2 at $t = 10$ s

Perturbation in Area 2.

In this state, the simultaneous coordination scheme is inspected with existence of both the FLAGC and CAGC under occurrence of 4 percent SLP in Area 2 which is triggered at $t = 10$ s. The system response with and without coordination scheme is displayed in Fig. 10. As expected, Fig. 10 portray the previous result.

Perturbation in Area 3.

Similar to two pervious subsections, the simultaneous coordination scheme is carried out whereas both the FLAGC and CAGC are available. The power system is also affected by occurrence of 5 percent SLP in Area 3 triggered at $t = 10$ s. The curves portrayed in Fig. 11 have transparently verified dynamic performance of FLAGC as compared with CAGC.

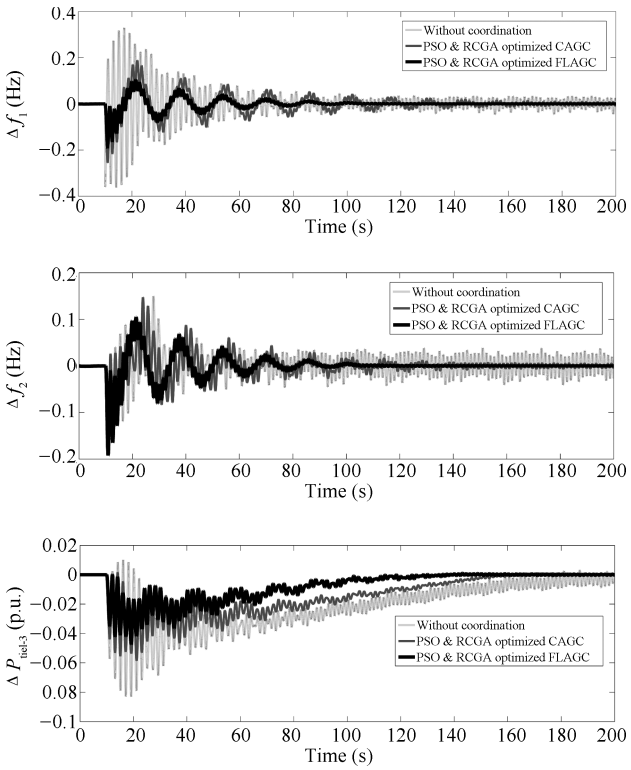

Fig. 11 Power system responses under 5 percent SLP in Area 3 at $t = 10$ s

5.2 Five-area thermal power system

This power system has been employed to better evaluation and verification of the studied scheme. What is done for three-area hydro-thermal power system, the efficiency of FLAGC has been evaluated under three conditions of SLP in all areas of thermal power system. One percent is taken into account as value of SLPs which are triggered at $t = 1$ s. The simultaneous coordinated scheme for both the FLAGCs and CAGCs is carried out by taking the (40) as fitness function. Optimized FLAGCs and CAGCs controllers′ parameters in accordance with simultaneously coordination scheme are presented in Tables 4 and 5.

The following sections have obviously endorsed the concluded results of the same, i.e., robust performance of FLAGC as compared with CAGC in coordination scheme aimed to suppress power system dynamic oscillations.

SLP in Area 1.

It is considered that 1 percent SLP occurred in Area 1 at the time of $t = 1$ s. Dynamic performance of both the FLAGC and CAGC has been appraised in the affected power system. Similar to previous section, both the PSO and RCGA have been executed to settle the optimization scheme. The simulation result is shown in Fig. 12 that clearly certified dynamic performance of FLAGC.

SLP in Area 2.

In this part, the occurrence of 1 percent SLP in Area 2 has affected the power system at $t = 1$ s. The curves portrayed in Fig. 13 have shown dynamic performance of FLAGC as compared to CAGC.

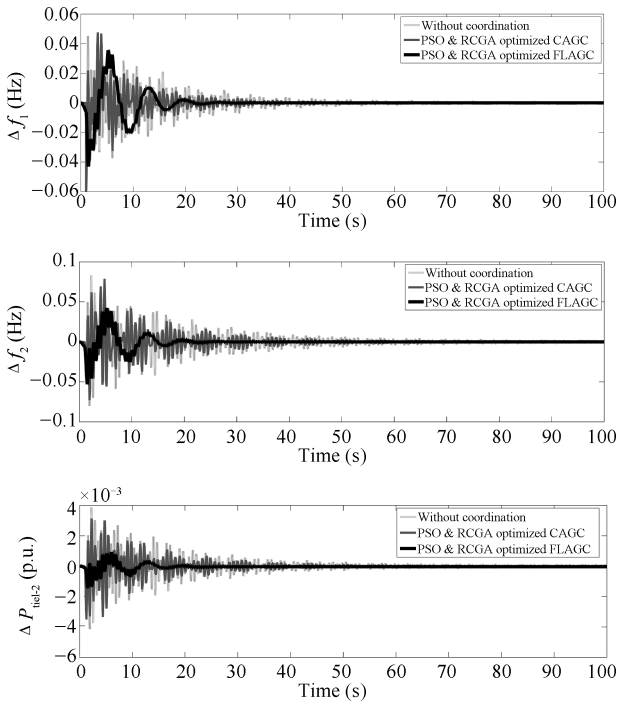

Fig. 12 Power system responses under 1 percent SLP in Area 1 at $t = 1$ s

Table 4 Optimal parameters of thermal system′s FLAGCs

Area 1		Area 2		Area 3		Area 4		Area 5	
K_{FP1}	K_{FI1}	K_{FP2}	K_{FI2}	K_{FP3}	K_{FI3}	K_{FP4}	K_{FI4}	K_{FP5}	K_{FI5}
0.005 9	0.620 5	0.039 6	0.311 4	0.002 9	0.313 7	0.031 0	0.194 1	0.022 4	0.895 8

Table 5 Optimal parameters of thermal system's CAGCs

Area 1		Area 2		Area 3		Area 4		Area 5	
K_{CP1}	K_{CI1}	K_{CP2}	K_{CI2}	K_{CP3}	K_{CI3}	K_{CP4}	K_{CI4}	K_{CP5}	K_{CI5}
0.021 9	3.781 2	0.059 8	3.165 3	0.021 4	1.264 0	0.021 2	3.940 0	0.055 2	0.058 8

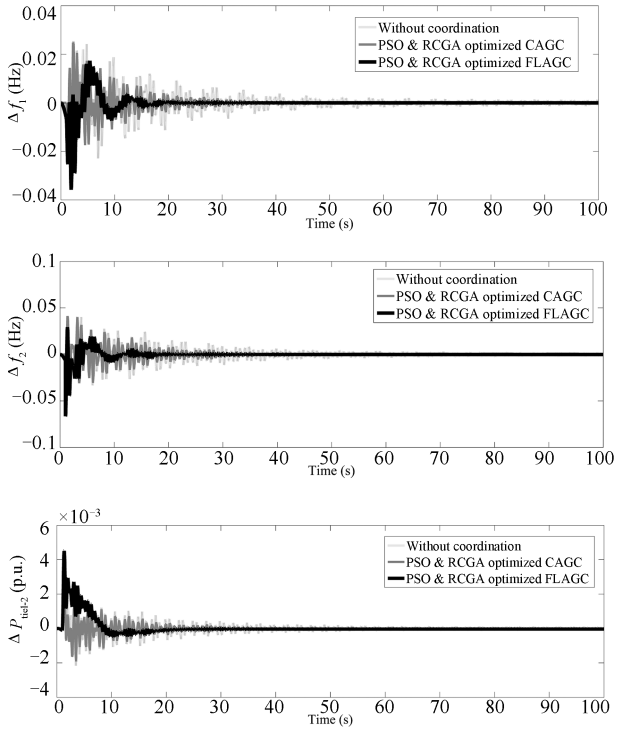

Fig. 13 Power system responses under 1 percent SLP in Area 2 at $t = 1$ s

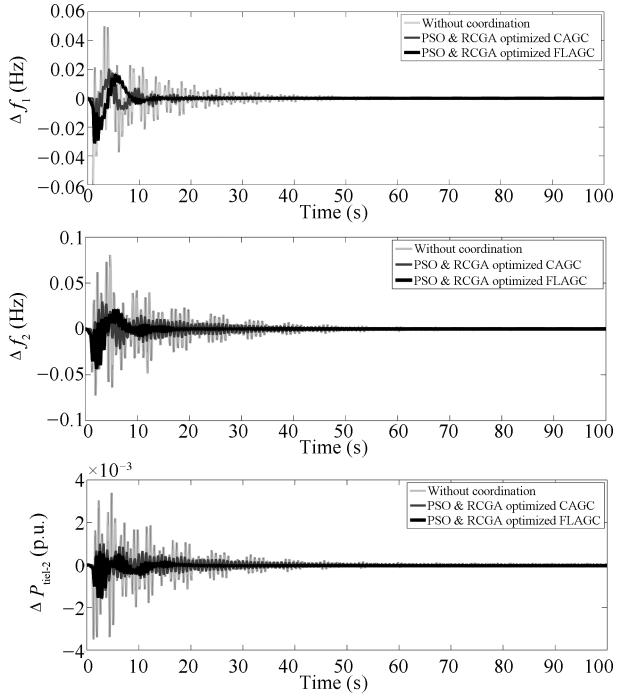

Fig. 14 Power system responses under 1 percent SLP in Area 3 at $t = 1$ s

SLP in Area 3.

The system response under occurrence of 1 percent SLP in Area 3 at $t = 1$ s is presented in Fig. 14. It is obvious that power system dynamic oscillations have been significantly suppressed by FLAGC. Thus, dynamic performance of FLAGC against CAGC is well proved.

SLP in Area 4.

One percent SLP is happened in Area 4 that is triggered at $t = 1$ s. The relevant curves resulted from this perturbation are presented in Fig. 15. FLAGC could appropriately suppress these oscillations and augment dynamic stability of five-area thermal power system.

SLP in Area 5.

Similar to four previous subsections, 1 percent SLP has affected the power system to evaluate dynamic performance of FLAGC. This perturbation is occurred in Area 5 at $t = 1$ s. The curves presented in Fig. 16 have transparently indicated FLAGC has outstanding dynamic performance as compared to CAGC.

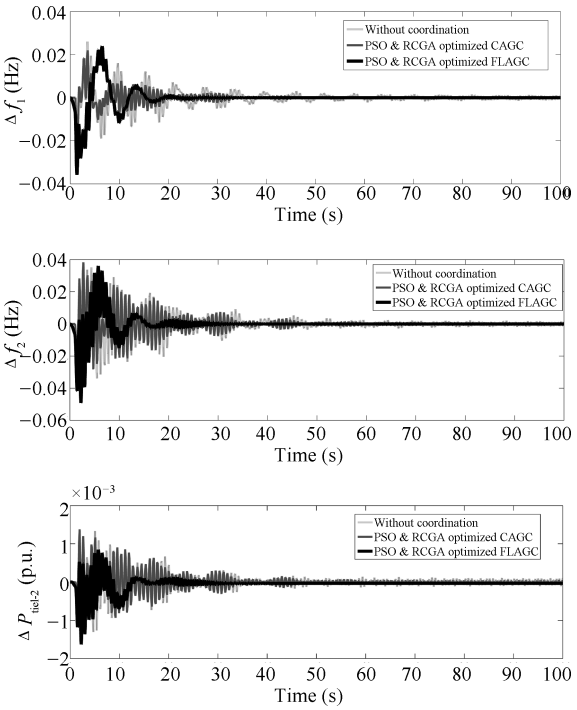

Fig. 15 Power system responses under 1 percent SLP in Area 4 at $t = 1$ s

6 Conclusions

In this paper, an effective and robust AGC based on fuzzy controller accompanied by a coordination scheme based on PSO and RCGA techniques is suggested to damp out the system frequency and tie-line power exchange deviations.

Hence, two different multi-area interconnected power systems have been taken into account to provide an appropriate bed in order to appraise and certify the performance of FLAGC. On the other hand, simultaneous coordination among both the FLAGCs and CAGCs has been scheduled for zeroing the ACE of each area of interconnected power system. The efficiency of this strategy has been significantly inspected by considering the SLP in both the studied power systems. Ultimately, the unveiled results have evidently endorsed the high performance of FLAGCs in order to suppress the power system oscillations as compared with CAGCs in each power system.

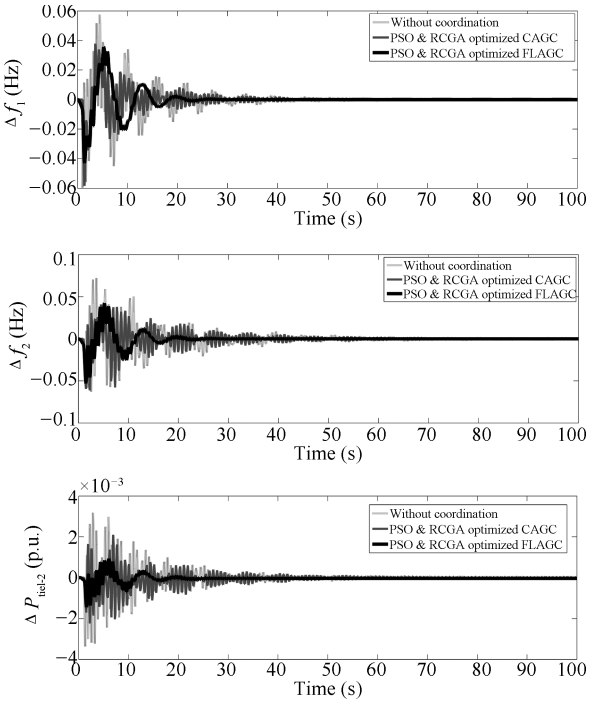

Fig. 16 Power system responses under 1 percent SLP in Area 5 at $t = 1$ s

Appendix

Three-area hydro-thermal power system:

$f = 60$ Hz, $T_{gi} = 0.08$ s, $T_{ri} = 10$ s, $H_i = 5$ s, $T_{ti} = 0.3$ s, $K_r = 0.5$, $P_{ri} = 2\,000$ MW, $T_{pi} = 20$ s, $K_d = 4.0$, $K_p = 1.0$, $K_i = 5.0$, $D_i = 0.008\,33$ p.u.MW/Hz, $K_{pi} = 120$ Hz/p.uMW.

Five-area thermal power system

Area 1: 2 000 MW, Area 2: 4 000 MW, Area 3: 8 000 MW, Area 4: 10 000 MW, Area 5: 12 000 MW. $f = 60$ Hz, $T_{gi} = 0.08$ s, $T_{ri} = 10$ s, $H_i = 5$ s, $T_{ti} = 0.3$ s, $K_r = 0.5$, $P_{tie-\max} = 200$ MW, $D_i = 0.008\,33$ p.u.MW/Hz, $T_{pi} = 20$ s, $K_{pi} = 120$ Hz/p.uMW, $T_{ij} = 0.544$, $T_w = 1.0$ s, $K_p = 1.0$, $K_d = 4.0$, $K_i = 5.0$.

References

[1] A. Kazemi, M. R. J. Motlagh, A. H. Naghshbandy. Application of a new multi-variable feedback linearization method for improvement of power systems transient stability. *International Journal of Electrical Power and Energy Systems*, vol. 29, no. 4, pp. 322–328, 2007.

[2] S. Ahmadi, H. Bevrani, S. Shokoohi, E. Hasanii. An improved droop control for simultaneous voltage and frequency regulation in an AC microgrid using fuzzy logic. In *Proceedings of the 23rd Iranian Conference on Electrical Engineering*, IEEE, Tehran, Iran, pp. 1486–1491, 2015.

[3] D. P. Iracleous, A. T. Alexandridis. A multi-task automatic generation control for power regulation. *Electric Power Systems Research*, vol. 73, no. 3, pp. 275–285, 2005.

[4] W. Tan, Z. Xu. Robust analysis and design of load frequency controller for power systems. *Electric Power Systems Research*, vol. 79, no. 5, pp. 846–853, 2009.

[5] A. D. Falehi, M. Rostami, A. Doroudi, A. Ashrafian. Optimization and coordination of SVC-based supplementary controllers and PSSs to improve power system stability using a genetic algorithm. *Turkish Journal of Electrical Engineering and Computer Sciences*, vol. 20, no. 5, pp. 639–654, 2012.

[6] P. Kundur, M. Klein, G. J. Rogers, M. S. Zywno. Application of power system stabilizers for enhancement of overall system stability. *IEEE Transactions on Power Systems*, vol. 4, no. 2, pp. 614–626, 1989.

[7] Y. G. Rebours, D. S. Kirschen, M. Trotignon, S. Rossignol. A survey of frequency and voltage control ancillary services – Part I: Technical features. *IEEE Transactions on Power Systems*, vol. 22, no. 1, pp. 350–357, 2007.

[8] S. Selvakumaran, V. Rajasekaran, R. Karthigaive. Genetic algorithm tuned IP controller for Load Frequency Control of interconnected power systems with HVDC links. *Archives of Electrical Engineering*, vol. 63, no. 2, pp. 161–175, 2014.

[9] I. Pan, S. Das. Fractional-order load-frequency control of interconnected power systems using chaotic multi-objective optimization. *Applied Soft Computing*, vol. 29, pp. 328–344, 2015.

[10] X. Li, X. P. Zhao, J. Chen. Controller design for electric power steering system using T-S fuzzy model approach. *International Journal of Automation and Computing*, vol. 6, no. 2, pp. 198–203, 2009.

[11] H. A. Yousef, M. Hamdy. Observer-based adaptive fuzzy control for a class of nonlinear time-delay systems. *International Journal of Automation and Computing*, vol. 10, vol. 4, pp. 275–280, 2013.

[12] H. G. Guo, B. J. Zhang. Observer-based variable universe adaptive fuzzy controller without additional dynamic order. *International Journal of Automation and Computing*, vol. 11, no. 4, pp. 418–425, 2014.

[13] P. S. Rao, I. Sen. Robust pole placement stabilizer design using linear matrix inequalities. *IEEE Transactions on Power Systems*, vol. 15, no. 1, pp. 313–319, 2000.

[14] M. A. Abido. Pole placement technique for PSS and TCSC-based stabilizer design using simulated annealing. *International Journal of Electrical Power and Energy Systems*, vol. 22, no. 8, pp. 543–554, 2000.

[15] B. C. Pal. Robust pole placement versus root-locus approach in the context of damping interarea oscillations in power systems. *IEE Proceedings – Generation, Transmission and Distribution*, vol. 149, no. 6, pp. 739–745, 2002.

[16] L. Rouco, F. L. Pagola. An eigenvalue sensitivity approach to location and controller design of controllable series capacitors for damping power system oscillations. *IEEE Transactions on Power Systems*, vol. 12, no. 4, pp. 1660–1666, 1997.

[17] M. E. Aboul-Ela, A. A. Sallam, J. D. McCalley, A. A. Fouad. Damping controller design for power system oscillations using global signals. *IEEE Transactions on Power Systems*, vol. 11, no. 2, pp. 767–773, 1996.

[18] S. Panda, N. P. Padhy. Optimal location and controller design of STATCOM for power system stability improvement using PSO. *Journal of the Franklin Institute*, vol. 345, no. 2, pp. 166–181, 2008.

[19] R. L. Haupt, S. E. Haupt. *Practical Genetic Algorithms*, 2nd ed., New York, USA: Wiley, 2004.

[20] A. M. El-Zonkoly, A. A. Khalil, N. M. Ahmied. Optimal tunning of lead-lag and fuzzy logic power system stabilizers using particle swarm optimization. *Expert Systems with Applications*, vol. 36, no. 2, pp. 2097–2106, 2009.

[21] A. D. Falehi, M. Rostami. A robust approach based on RCGA-optimization technique to enhance power system stability by coordinated design of PSS and AVR. *International Review of Electrical Engineering*, vol. 6, no. 1, pp. 371–378, 2011.

[22] H. Shayeghi, A. Safari, H. A. Shayanfar. PSS and TCSC damping controller coordinated design using PSO in multi-machine power system. *Energy Conversion and Management*, vol. 51, no. 12, pp. 2930–2937, 2010.

[23] Q. Gu, A. Pandey, S. K. Starrett. Fuzzy logic control schemes for static VAR compensator to control system damping using global signal. *Electric Power Systems Research*, vol. 67, no. 2, pp. 115–122, 2003.

[24] O. I. Elgerd, C. E. Fosha. Optimum megawatt-frequency control of multiarea electric energy systems. *IEEE Transactions on Power Apparatus and Systems*, vol. PAS-89, no. 4, pp. 556–563, 1970.

[25] A. Khodabakhshian, R. Hooshmand. A new PID controller design for automatic generation control of hydro power systems. *International Journal of Electrical Power and Energy Systems*, vol. 32, no. 5, pp. 375–382, 2010.

[26] W. Tan. Tuning of PID load frequency controller for power systems. *Energy Conversion and Management*, vol. 50, no. 6, pp. 1465–1472, 2009.

[27] J. Kennedy, R. Eberhart. Particle swarm optimization. In *Proceedings of the IEEE International Conference on Neural Networks*, IEEE, Perth, USA, pp. 1942–1948, 1995.

[28] J. Kennedy, R. C. Eberhart, Y. H. Shi. *Swarm Intelligence*, San Francisco, USA: Morgan Kaufmann Publishers, 2001.

[29] S. Shojaeian, E. S. Naeeni, M. Dolatshahi, H. Khani. A PSO-DP based method to determination of the optimal number, location, and size of FACTS devices in power systems. *Advances in Electrical and Computer Engineering*, vol. 14, no. 1, pp. 109–114, 2014.

[30] A. D. Falehi, M. Rostami, H. Mehrjardi. Transient stability analysis of power system by coordinated PSS-AVR design based on PSO technique. *Engineering*, vol. 3, pp. 478–484, 2011.

[31] L. C. Saikia, J. Nanda, S. Mishra. Performance comparison of several classical controllers in AGC for multi-area interconnected thermal system. *International Journal of Electrical Power and Energy Systems*, vol. 33, no. 3, pp. 394–401, 2011.

[32] K. C. Divya, P. S. Nagendra Rao. A simulation model for AGC studies of hydro-hydro systems. *International Journal of Electrical Power and Energy Systems*, vol. 27, no. 5–6, pp. 335–342, 2005.

[33] S. P. Ghoshal. Optimizations of PID gains by particle swarm optimizations in fuzzy based automatic generation control. *Electric Power Systems Research*, vol. 72, no. 3, pp. 203–212, 2004.

[34] P. Kundur. *Power System Stability and Control*, New York, USA: McGraw-Hill, 1994.

[35] A. D. Falehi, M. Rostami. Design and analysis of a novel dual-input PSS for damping of power system oscillations employing RCGA-optimization technique. *International Review of Electrical Engineering*, vol. 6, no. 2, pp. 938–945, 2011.

Ali Darvish Falehi received the M. Sc. degree from the Shahed University, Iran in 2010. He is currently a Ph. D. degree candidate at Shahid Beheshti University, Iran. He has published more than 10 ISI papers like *IET Generation, Transmission & Distribution, SPRINGER Frontiers of Information Technology & Electronic Engineering, Journal of Intelligent and Fuzzy Systems* and *Turkish Journal of Electrical Engineering and Computer Sciences*.

His research interests include FACTS, D-FACTS, power system stability, power quality, artificial intelligence and controller design.

E-mail: falehi87@gmail.com; a-darvishfalehi@sbu.ac.ir (Corresponding author)

ORCID iD: 0000-0002-8333-0114